Journal of Colloid and Interface Science xxx (2011) xxx–xxx

Contents lists available at SciVerse ScienceDirect

Journal of Colloid and Interface Science

www.elsevier.com/locate/jcis

Synthesis of mesoporous silicas in alkaline and acidic media using the systems cetyltrimethylammonium tosylate (CTAT)–Pluronic F127 triblock copolymer and CTAT–Pluronic F68 triblock copolymer as templates

Maximiliano Brigante *, Pablo C. Schulz

INQUISUR, Departamento de Química, Universidad Nacional del Sur, Av. Alem 1253, 8000 Bahía Blanca, Argentina

ARTICLE INFO

Article history:
Received 1 September 2011
Accepted 22 November 2011
Available online xxxx

Keywords:
Mesoporous silica materials
Synthesis
Cetyltrimethylammonium tosylate
Pluronic F127
Pluronic F68
Triblock copolymer–CTAT interactions

ABSTRACT

Mesoporous silica materials were synthesized in alkaline and acidic media, using cetyltrimethylammonium tosylate (CTAT), Pluronic triblock copolymers F127 and F68, and mixtures of CTAT with each copolymer in order to investigate the effects of pH, surfactant concentration, and CTAT/triblock copolymer molar ratios on the morphology and texture of the synthesized materials. The results show that the kind of mesoporous materials and their pore size can be tuned by changing not only the pH but also the proportion of components and the nature of the copolymer. In alkaline synthesis, microscopic bicontinuous materials are obtained, which are composed by nanoscopic plate-like particles having slit-shaped pores. In acidic synthesis, on the contrary, monolithic silicas are obtained. These materials are also composed by nanoscopic plate-like particles having slit-shaped pores, although in some cases, the microscopic structures are formed by fused spherical particles. The inclusion of the triblock copolymer in the template composition causes a transformation from a bimodal to a monomodal pore size distribution, leading to small and nearly round pores which are probably formed by copolymer or copolymer-CTAT mixed micelles. The differences between the systems synthesized by CTAT–Pluronic F127 and CTAT–Pluronic F68 are explained on the basis of the different interactions between each copolymer and CTAT.

1. Introduction

Micelle-templated mesoporous silica materials are rapidly becoming important in many fields of chemistry for hosting reactants or catalysts in confined space. The properties of the materials are used in catalysis, separation, drug delivery, chemical sensing, optic and electronic applications, reinforcing of rubber and as templates in the synthesis of nanomaterials [1,2]. Fine control of the pore size, wall structure, surface functionalization, defects, and morphology is needed for fine-tuning the pores as nanoreactors [3,4].

Many research groups have investigated different surfactant-silica chemistry systems that yield various shapes including spherical beads, gyroids, ropes, toroids, ellipsoids, shells, knots, helical structures, as well as thin films, fibers and monoliths, depending on the synthesis conditions [1,5–7]. Among the numerous synthesis parameters that determine the synthesis mechanism, the morphology, and the texture of the resulting materials, the nature of the surfactant template, the pH, the concentration of the reactants in the aqueous medium, the presence of a co-surfactant and/or co-solvent, the temperature, the stirring, as well as the procedure used for the mixing of the reactants or for the heating stage can be mentioned (i.e., in one or two steps) [1,4,8]. Unfortunately, in most reports, the effects of the synthesis conditions on the characteristics of the final material are investigated separately and could result in erroneous results or misleading conclusions because the synthesis system generally behaves differently under different synthesis conditions.

In 1998, Zhao et al. [9,10] proposed a new synthesis method of ordered mesoporous silica by using the amphiphilic triblock poly(ethylene oxide)–poly(propylene oxide)–poly(ethylene oxide) copolymers (PEO_n–PPO_m–PEO_n), known as Poloxamers or Pluronics, as the structure-directing agent in acidic medium. These novel mesoporous materials were denoted SBA-n silicas and exhibit two and three-dimensional hexagonal (SBA-12, 3, 15) [9–11] and cubic (SBA-1, 6, 16) pore architectures [12]. Although the details of the mechanism are much less clear than those for the synthesis of the M41S-type silica materials under basic conditions, it is still understandable that these copolymers show the ability to form liquid–crystalline structures, where the ethylene oxide (EO) units and the cationic silicate species favorably interact to form the mesostructured assembly, and the mesoporous silica materials can be synthesized by synergistic self-assembly between surfactant and silica species to form mesoscopically ordered structures [12]. Moreover, the use of these compounds to obtain ordered inorganic porous matrices is the most promising route for high porosity, large pore dimension, low cost, and low toxicity [13].

* Corresponding author.
E-mail address: brigante@uns.edu.ar (M. Brigante).

0021-9797/$ - see front matter © 2011 Elsevier Inc. All rights reserved.
doi:10.1016/j.jcis.2011.11.056

Several reports exist in literature about the assembly pathways between the non-ionic triblock copolymer micelles and the silica precursor for synthesizing a mesoporous material. At pH below the isoelectric point of silica (pH < 2), the electrostatic assembly route is believed to be $(N^0H^+)(X^-I^+)$, where N^0H^+ is the surfactant hydrogen bonded to a hydronium ion, X^- is the halide ion or counterion, and I^+ is the protonated silica [9,10,14]. At pH ~ 2, the electrostatic interaction between the silica species and the copolymer molecules is negligible because the surface charge of silica is near zero [14]. At pH > 2, on the contrary, the silica species in aqueous solutions are negatively charged due to the deprotonation of silanol groups [15]. Therefore, the electrostatic assembly mechanism at pH > 2 may be $N^0H^+I^-$, where the protonated micelles interact directly with negatively charged silica species (I^-). On the other hand, Qi et al. [16] suggested that an alternative complex pathway can occur if a cationic surfactant (S^+), acting as a co-surfactant, is present in the triblock copolymer template at pH < 2. This involves both $S^+X^-I^+$ and $(N^0H^+)(X^-I^+)$ assemblies at the interface of mixed micelles. However, the mentioned mechanism is still not understood and requires further investigations.

Recently, we have reported the aggregation and adsorption at the air–solution interface of the cationic surfactant cetyltrimethylammonium p-toluene sulfonate or tosylate (CTAT) with two Pluronics triblock copolymers, F68 and F127, at several CTAT/Pluronic molar ratios [17]. CTAT was chosen for such studies because it presents interesting rheological properties and relatively low critical micelle concentration (CMC) and critical rod-like concentration (CRC): 0.24–0.26 and 1.90 mM for the CMC and the CRC at room temperature, respectively [18,19]. We clearly showed that the behavior in both system mixtures, i.e., CTAT–F127 and CTAT–F68, was strongly dependent on the nature of the copolymer amphiphile, and differences in length in the hydrophobic and hydrophilic chains may cause different behaviors. However, and as far as we know, there is not information in the literature on the silica synthesis by using these mixtures.

Thus, and in order to continue with the investigations mentioned above, the aim of this article is to present a study of the hydrothermally synthesis of mesoporous silica materials, in acidic and alkaline media, by reaction of precursors prepared by CTAT mixed with Pluronic F127 and F68 solutions. Our research will therefore focus on the effect of the pH and the interaction of the mentioned surfactants with the silica precursor, relevant parameters (not the only ones) that control the synthesis mechanism, and structural and texture properties of the resulting materials. All these parameters were analyzed and compared as a function of synthesis pH, CTAT concentration, and CTAT/triblock copolymer molar ratios.

2. Materials and methods

Cetyltrimethylammonium tosylate (CTAT, MW = 455.7 $gmol^{-1}$), Pluronic triblock copolymers F68 ($PEO_{76}PPO_{29}PEO_{76}$, MW = 8400 $gmol^{-1}$) and F127 ($PEO_{97}PPO_{69}PEO_{97}$, MW = 12,600 $gmol^{-1}$), and tetraethylorthosylicate (TEOS) were purchased from Sigma–Aldrich. NaOH and HCl (37% concentration) were obtained from Anedra. All chemicals were of analytical grade and used as received. Doubly distilled water was used for the preparation of solutions.

Mesoporous silica materials were prepared using a procedure similar to that described by Messina et al. [20]. Briefly, 11.6 mL of TEOS were mixed with 2 mL of water and stirred for 10 min at 500 rpm. Then, a solution formed by 1.1 g of NaOH in 20 mL water was added drop by drop to the TEOS solution under stirring. At the same time, 38 mL of CTAT–Pluronic F68 (or CTAT–Pluronic F127) mixed solutions was prepared with different molar ratios by adding the desired amounts of surfactants to water. The mixtures were stirred in an autoclave flask at 35 °C to form a transparent template solution, and then, they were left at room temperature. To obtain the mesoporous material in alkaline media, the surfactant solution was added 2 min after the addition of the NaOH solution. The resulting gel was stirred for 5 min and then left for 48 h in an autoclave at 100 °C. After this, the gel was filtered and washed with distilled water and left to dry at room temperature. Finally, it was calcined in an air flux by increasing the temperature from room temperature to 540 °C with a heating rate of 2 °C min^{-1} and holding for 7 h at 540 °C.

The synthesis of the mesoporous silica in acidic medium was carried out in similar conditions as described above except that the NaOH solution was substituted by 20 mL of solution containing 1.04 g of HCl. Table 1 summarizes the final molar gel compositions and structural properties of the obtained products.

The synthesized silica materials were characterized by the techniques usually employed in porous materials, such as scanning and transmission electron microscopy and the N_2-BET method for surface area (A_{BET}), pore volume ($V_{BJHdepv}$), and pore diameter (D_{aBJH}) determination. Scanning electron microscopy (SEM) was performed using a LEO 40-XVP microscope equipped with a secondary electrons detector. The samples were prepared on graphite stubs and coated with a ca. 300 Å gold layer in a PELCO 91,000 sputter coater. Transmission electron microscopy (TEM) was performed using a JEOL 100 CX II transmission electron microscope, operated at 100 kV with magnification from 50,000× to 200,000×. Observations were made in a bright field. Powdered samples were placed on copper supports of 2000 mesh. The nitrogen adsorption isotherms at 77.6 K were measured with a Micrometrics Model Accelerated Surface Area and Porosimetry System (ASAP) 2020 instrument. Each sample was degassed at 373 K for 720 min at a pressure of 1×10^{-4} Pa.

3. Results and discussion

3.1. Alkaline synthesis of silica materials using pure CTAT as template

Fig. 1 shows the pore size distribution of materials synthesized using CTAT solutions as template. Both materials synthesized in an alkaline medium, i.e., S1 and S2, show two maxima, one at 1.90 ± 0.34 nm and the other at 1.00 ± 0.41 nm. There is also a broad distribution of pore sizes above these peaks. This is also reflected in the BJH average pore diameters obtained in the analysis of the nitrogen sorption isotherms (D_{aBJH} = 8.90 nm (S1) and 10.10 nm (S2)).

Fig. 2 shows the electron micrographs of S1 and S2. Both samples have a microscopic bicontinuous structure with different pore sizes (Fig. 2a). At a higher magnification, the bicontinuous structure is formed by silica spheres (Fig. 2b). TEM micrograph (Fig. 2c) shows that the structure of silica globules is formed by an agglomeration of lamellae, indicating that probably the liquid crystal formed during the synthesis that acted as template was lamellar instead of hexagonal, which is formed by this surfactant in pure water [21].

The nitrogen adsorption–desorption isotherms of S1 and S2 are shown in Fig. 3. Both samples show typical type IV isotherms, which are characteristic of many mesoporous industrial adsorbents.

The hysteresis loops are type H3, typical of plate-like particles giving rise to slit-shaped mesopores in agreement with the TEM observations [22]. The beginning of the almost linear middle region of the isotherm (point B) is often taken to indicate the stage at which monolayer coverage is complete and multilayer adsorption about to begin. It may be seen that in S2 isotherm, the position of B is higher than in S1, which is reflected by the surface area values: 94.02 $m^2 g^{-1}$ (S1) and 261.80 $m^2 g^{-1}$ (S2) [22].

The main data obtained from nitrogen sorption isotherms and from SEM and TEM are shown in Table 1 and in the Supporting

Table 1
Molar gel compositions and structural properties of synthesized materials.

Sample denomination	Gel composition	Pore radius[a] (nm)	A_{bet} ($m^2\ g^{-1}$)	D_{aBJH} (nm)	$V_{BJHdepv}$ ($cm^3\ g^{-1}$)
Pure CTAT as template					
SI	0.53NaOH:0.011 CTAT	1.91 ± 0.34/1.17 ± 0.41	94.02	8.90	0.177
S2	0.53 NaOH:0.055 CTAT	1.91 ± 0.34/0.84 ± 0.41	261.80	10.10	0.355
S3	1 TEOS:0.53 HCl:0.011 CTAT	2.90 ± 1.10	544.30	1.35	0.692
CTAT–Pluronic F127 as template					
S4	1 TEOS:0.53NaOH:0.011 CTAT:0.0012 F127	1.90 ± 0.88	18.23	16.70	0.062
S5	1 TEOS:0.53NaOH: 0.011CTAT:0.0037F127	1.74 ± 1.09	145.90	8.56	0.328
S6	1 TEOS:0.53NaOH:0.011 CTAT:0.011 F127	1.94 ± 0.76	160.20	8.58	0.375
S7	1 TEOS:0.53 NaOH:0 CTAT:0.011 F127	2.00 ± 1.70	100.40	10.10	0.271
S8	1 TEOS:0.53 HCl:0.011 CTAT:0.0037F127	1.80 ± 0.73	601.40	1.77	0.520
S9	1 TEOS:0.53 HC1: 0.011 CTAT:0.011 F127	2.00 ± 0.73	551.10	2.04	0.579
S10	1 TEOS:0.53 HC1:O CTAT:0.011 F127	1.92 ± 0.73	506.30	1.95	0.507
CTAT–Pluronic F68 as template					
S11	1 TEOS:0.53NaOH:0.011 CTAT:0.0012 F68	1.73 ± 0.35	115.10	7.29	0.214
S12	1 TEOS:0.53NaOH:0.011 CTAT:0.0037F68	1.32 ± 0.34	325.40	4.22	0.419
S13	1 TEOS:0.53NaOH:0.011 CTAT:0.011 F68	1.91 ± 0.70	199.60	4.18	0.252
S14	1 TEOS:0.53 NaOH:0 CTAT:0.011 F68	1.92 ± 0.35	127.70	9.63	0.326
S15	1 TEOS:0.53HC1:0.011 CTAT:0.0037 F68	1.85 ± 0.69	574.50	2.85	0.436
S16	1 TEOS:0.53HC1:0.011 CTAT:0.011 F68	2.05 ± 1.00	734.30	3.23	0.619
S17	1 TEOS:0.53 HC1:O CTAT:0.011 F68	1.74 ± 0.59	775.30	3.40	0.689

Note: A_{BET}: BET surface area; D_{aBJH}: BJH adsorption average pore diameter; $V_{BJHdcpv}$: desorption cumulative volume of pores.
[a] Obtained from the pore size distribution plot.

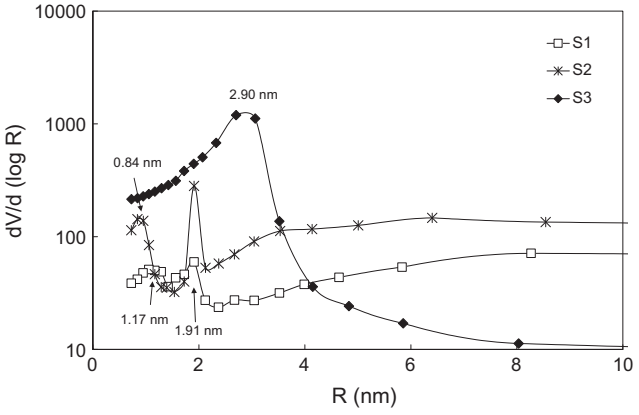

Fig. 1. Pore size distribution of the materials synthesized with CTAT.

Material, SM, respectively (see SM Table S1). Table 1 shows that the surface area and pore volume of S1 and S2 are moderate and increase with an increase in the CTAT concentration. Similar results were reported by Lenlong et al. [23] for the system cetyltrimethylammonium bromide (CTAB)–TEOS. The authors explained the increase in surface area as follows: at low CTAB concentration, rods surrounded by several layers of silica form and aggregate into organic–inorganic cylinders yielding a 2D structure. At higher concentrations, the corresponding amount of silica precursor per surfactant molecule falls down drastically and condenses around the cylindrical micelles formed by the organic molecules leading to a decrease in the thickness of the silica pore walls and thus to an increase in the surface area.

In spite of the mentioned above, the results obtained in this work clearly show that both external organization and internal pore structure are governed by the presence of alkali or acid in the reaction system. This was also found by other authors and is attributed to the effect on the surfactant packing parameter by the interaction between the surfactant head group and the silanolate or charged silanol ($Si–O^-$ or $Si—OH_2^+$) at the interface of aggregates [4]. High silica surface charge-neutralizing surfactant charges, resulting in lower surface area per head group, lead to higher V/la_0 values, where V is the volume of the surfactant hydrophobic tail, l is the surfactant tail length, and a_0 is the area per surfactant head group.

In synthesis processes, there are at least three kinds of charged species in solution: silica species (I^- or I^+), cationic surfactant (S^+), and its counterion (X^-). Their interactions depend on the silicate oligomeric species present because their charge densities depend on the degree of oligomerization. With enough strong interaction, the silicate ions exchange onto the micellar interface, and the local enriched concentration results in accelerated condensation of the silicate species. In alkaline conditions, the anionic silicate species condense at the surface of the cationic surfactant through strong Coulomb interactions (S^+I^-). There is a competition between I^- and X^- species to bind the micelles surface, and the particularly, strong interaction of tosylate with micelles can affect the results in comparison with, e.g., CTAB. The increasing rate of formation of the mesostructure is related to the increasing hydrophobicity of the counterion [4]. The more strongly adsorbing X^- would block the adsorption of silicate ions on micelles and delay the formation of the silica-surfactant mesophases. This, in turn, affects the structure of the synthesized material. Tosylate ions are strongly adsorbing counterions, i.e., the CTAT micelle ionization degree is about 0.1 [17].

Alkyltrimethylammonium bromide-silicate systems tend to form a lamellar phase at room temperature for $n \geqslant 18$ and pH $\geqslant$ 11, where n is the number of carbon atoms in the alkylic chain. For the CTAB ($n = 16$)–sodium silicate system, Liu et al. reported that MCM-48 could be made by simply controlling the alkalinity [24] instead of MCM-41, which is formed by hexagonal liquid crystals. Higher pH leads to MCM-48 of lower curvature structure, which is commonly associated with lamellar liquid crystals. Moreover, Gallis and Landry [25] reported that when ethanol molecules are present in enough large amounts (either added or produced in hydrolysis of TEOS) in high pH conditions, the cubic structure of MCM-48 can be made by using CTAB. Then, this phenomenon may also cause the production of low-curvature structures in the template aggregates.

Since at CTAT critical micelle concentration ($CMC_{CTAT} = 0.24 \pm 0.02$ mM) [17] spherical micelles form, while at the second CMC (3.82 mM) rod-like micelles appear [21], it may be supposed that the probable structure of the mesoporous silica will be that of MCM-41. The transition from spherical to rodlike micelles appears

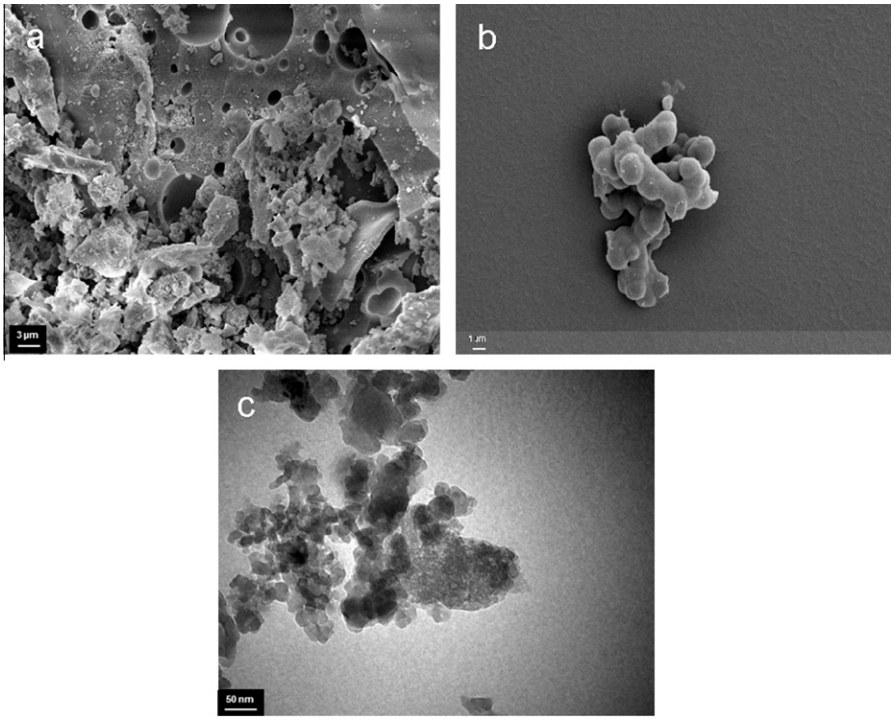

Fig. 2. Electron micrographs of materials synthesized with CTAT: (a) SEM micrograph of S2, showing the bicontinuous structure (magnitude = 5000×); and (b) SEM micrograph of S1, showing the globular structure (10,000×); and (c) TEM micrograph of S1, showing small platelets (200,000×).

to be relatively sharp at 1.90 mM, as revealed by static light scattering [18] and transition from Newtonian to shear thickening behavior of the solutions [26]. The wormlike micelles of this surfactant can grow to be sufficiently large to associate forming cooperative networks similar to those formed by entangled polymers above their coil-overlap concentration [27]. Moreover, these systems may exhibit viscoelastic behavior, similar to high molecular weight polymers in solution. The length of the wormlike micelles is affected by temperature, ionic strength of the solution, and the presence of other interacting components [28]. However, the system produces a mesoporous material which has the characteristics of a lamellar structure, with slit-shaped pores. The lamellar structure on the TEOS/CTAT/NaOH system was also reported by Mendoza et al. [29]. Then, it can be concluded that the alkaline conditions produce a reduction in the curvature of the surfactant aggregates as in the CTAB case. Both the bicontinuous microscopic structure and the lamellar nanoscopic one are caused by the formation of low-curvature surfactant aggregates.

Moreover, sulfonic acid is a strong acid, and then, its ionization is probably scarcely affected by the alkaline medium. However, the alkyltrimethylammonium group is a relatively weak base ($pK_b = 2.98$ at 25 °C [30]). Then, the interaction between tosylate and I^+ is probably not affected by changing the medium from acid to alkaline, but the interaction between I^+ and CTA^+ is probably affected reducing the repulsion between the two species. This situation can also affect the kind of mesophase formed as template in the silicate synthesis.

3.2. Acidic synthesis of silica materials using pure CTAT as template

As shown in Fig. 1, the pore size distribution of the material synthesized in acidic medium (S3) is completely different from those of the S1 and S2 samples. There is a unique broad peak at 2.90 ± 1.10 nm. It does not seem to appear a large pore size distribution as in the S1 and S2 samples. Fig. 4 shows the general characterization of S3. SEM micrographs show monolithic structures formed by spheres whose average diameter was 2.26 ± 0.35 µm (Fig. 4a and b). However, not all the material is formed by these spheres. At a nanoscopic level, the material is formed by small platelets with slit pores of variable size among them (Fig. 4c). The nitrogen sorption isotherm is also of type IV but the hysteresis loop is H2 (Fig. 4d), which corresponds to a non-defined distribution of pore sizes and shapes, which appears in several inorganic oxide gels and glasses. It was attributed in the past to "ink bottle pores", but it is now recognized that this provides an oversimplified picture and the role of network effects must be taken into account [22]. The surface area is rather high (544.3 $m^2\ g^{-1}$), and the average pore diameter is low (1.35 nm), indicating that larger pores are scarce. The pore volume is also high (0.692 $cm^3\ g^{-1}$).

Similar results were obtained in acidic conditions using Triton X-100 as a template [31]. The formation of spheroidal particles at low pH was attributed to a weak control of structure by micelles. Moreover, at very low pH, in the first step of the formation of the mesoporous silica, when the concentration of the surfactant is high, its micelles control more or less the polycondensation of the silicic acid, giving rise to discrete particles. In the second step, when the surfactant concentration becomes lower, this control weakens and a less organized gel-like or glassy material appears in which the particles formed in the first step are embedded. This glassy material acts as glue between the particles [31].

Moreover, in acidic synthesis below the isoelectric point of silica, the cationic silica precursor (I^+) formed at pH < 2 combines with S^+X^--type active sites in the surfactant aggregates through a weaker electrostatic interaction throughout a bridge counterion at the interface between surfactant and silica ($S^+X^-I^+$) [32]. This affects the structure order. It is usually softer than that in alkaline conditions. Generally, because of the weaker interaction between surfactant and silicas in acidic conditions, the original liquid crystalline phase is preserved when mixed with silica sources. The formation of lamellae in acidic conditions in the CTAT–TEOS system may be due to the strong hydrophobic interaction between cetyltrimethylammonium cation and the tosylate anion, causing a

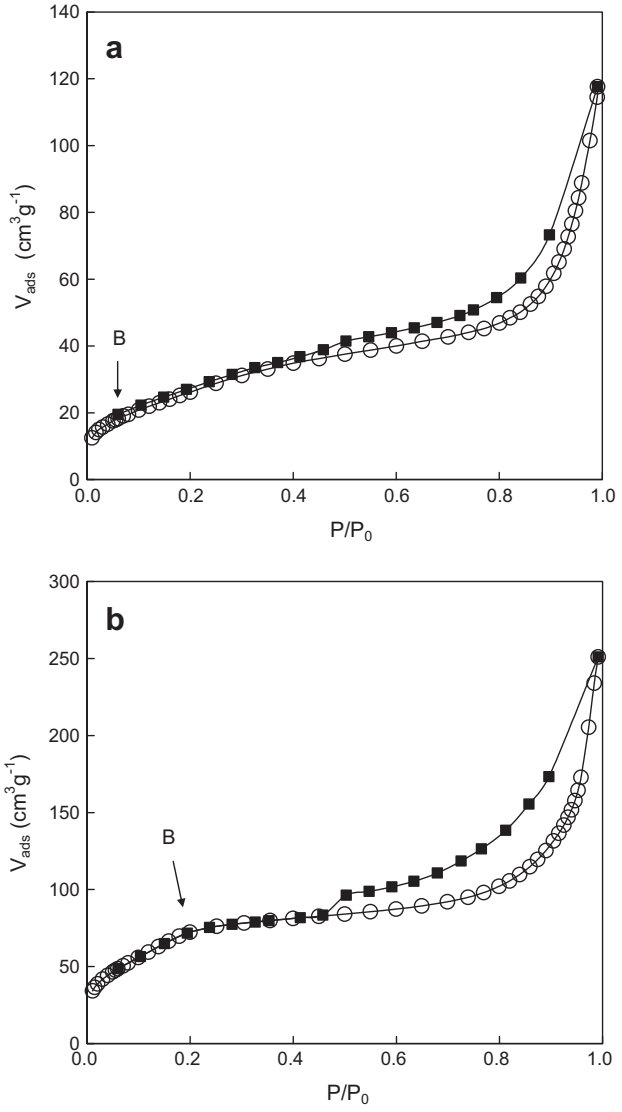

Fig. 3. Nitrogen sorption isotherms on (a) S1 and (b) S2. Open circles, adsorption; solid squares: desorption.

reduction of the packing parameter similar to the one produced by alkali.

Then, microscopic spheroidal particles are formed in the first step of polymerization, which are subsequently agglomerated creating the monoliths. The formation of small platelets at nanoscopic scale may be originated in a reduction of the packing parameter caused by the strong hydrophobic interaction between cetyltrimethylammonium cation and the tosylate anion in the presence of silica precursors.

3.3. Alkaline synthesis of silica materials using CTAT–Pluronic F127 system as template

Fig. 5 shows the pore size distribution of samples synthesized by mixtures of CTAT and Pluronic F127 in alkaline conditions. As it can be seen, the inclusion of Pluronic F127 in the system produces a change from the bimodal pore size distribution of the mesoporous silica produced with pure CTAT to a broad monomodal distribution of mesopores. Table 1 and SM Table S2 show the main data obtained from nitrogen adsorption isotherms, and SEM and TEM, respectively.

Fig. 6 shows the electron micrographs of samples synthesized with CTAT–Pluronic F127 mixed micelles as template. SEM micrographs show that the bicontinuous (sponge–like) structure is maintained but the increase in Pluronic F127 content reduces the pore size. However, in the system synthesized with the pure triblock copolymer (Figs. 6e), the bicontinuous structure is formed by rods producing irregular and very polydisperse pores.

In literature, a mesoporous silica synthesized with a cubic mesophase of Pluronic F127 in alkaline conditions gave a material having A_{BET} = 740 $m^2 g^{-1}$, D_{aBJH} = 5.40 nm, and $V_{BJHdepv}$ = 0.45 $cm^3 g^{-1}$ and whose microscopic structure was formed by ropelike aggregates [10]. Our material has lower surface area and pore volume, but higher pore size (see Table 1) and maintains the microscopic structure. The differences may be caused by the dissimilar concentration of the template and the unlike gelation conditions. On the other hand and according to the TEM micrographs, all samples show small porous platelets, with nearly round pores having a diameter of about 1.70 nm. These pores are absent in the pure CTAT system.

The nitrogen adsorption–desorption isotherms of samples synthesized by mixtures of CTAT and Pluronic F127 are shown in Fig. 7. The isotherms are type IV with a H3 hysteresis loop. These isotherms are similar to those found in aluminosilicate MCM-41 synthesized with cetyl and tetradecyltrimethylammonium bromides as templates [33]. As shown in Fig. 7a, different zones of the isotherm can be interpreted. The rise from points E to A represents the gradual condensation of nitrogen in the defects and external surface. The adsorption step F–E is interpreted as a stepwise multilayer adsorption on a uniform non-porous surface. The step-height represents the monolayer capacity for each adsorbed layer [22]. Upon descending, the rapid decrease from A to C reflects the macropore of interparticle voids. At point C, there is a cooperative evaporation from channels interconnecting the interparticle voids. The step between points E and F corresponds to the capillary desorption of mesopores [33]. This is congruent with the bicontinuous microscopic structure and the slit-shaped mesoporous. Similar isotherms were found in S4 and S5 (data not shown) and in MCM-41 materials having a unimodal mesopores size distribution and a broad microscopic pore size distribution [23]. The nitrogen sorption isotherm for S7 (Fig. 7b) differs from S6; i.e., it has not step C.

The morphology of the obtained materials may be influenced by the peculiar interaction between CTAT and the triblock copolymers. In a previous work [17], we studied the CTAT–Pluronic F127 mixed micelles. In the mentioned system, there is a monotonically repulsive interaction between the components. The aggregate structure differs from both the pure CTAT and the pure Pluronic F127 micelles at all proportions. The process for CTAT inclusion in the copolymer is initially gradual but above $\alpha_{CTAT} \approx 0.40$ (α_{CTAT} being the mole fraction of CTAT in the surfactant mixture), it is rapid and reaches saturation with $n_{CTAT} \approx 8.1$, where n_{CTAT} is the number of CTAT molecules by copolymer molecule, which is probably accompanied by a structure change in mixed micelles. Cyclic voltammetry measurements [34] indicate a strong reduction in the hydrodynamic radius (R_h) of mixed aggregates (about one order of magnitude) in this situation, which probably indicates the replacement of mixed micelles by complexes of one copolymer molecule with some CTAT ones. The inclusion of Pluronic molecules in mixed micelles produces a large increment of the aggregateś ionization degree α, which is caused by the separation between trimethylammonium groups, thus reducing the surface potential of the mixed micelles. In the systems here used, mixed micelles are saturated with CTAT and the ionization degree is high. For S4, α_{CTAT} = 0.90 and α = 0.62, for S5, α_{CTAT} = 0.85 and α = 0.75, and for S5, α_{CTAT} = 0.50 and α = 0.72.

Moreover, the polyoxyethylene chains interact via hydrogen bonding with the inorganic matrix. In high acid concentration,

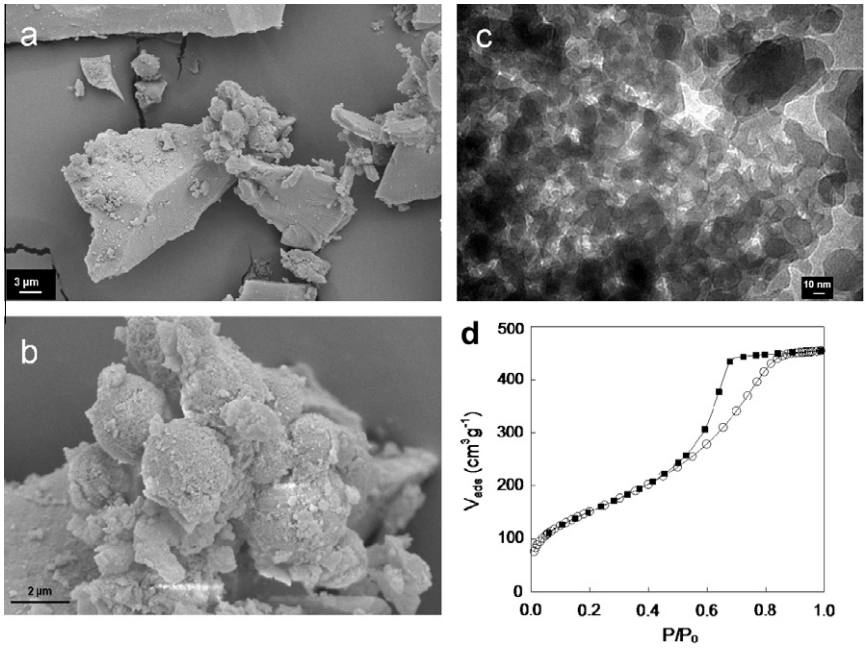

Fig. 4. General characterization of the sample S3: (a) SEM micrograph at 5000×, showing the monolithic structure; (b) SEM micrograph at 20,000×, showing the globular structure of monoliths; (c) TEM micrograph at 450,000×; and (d) nitrogen sorption isotherms. Open circles, adsorption; solid squares, desorption.

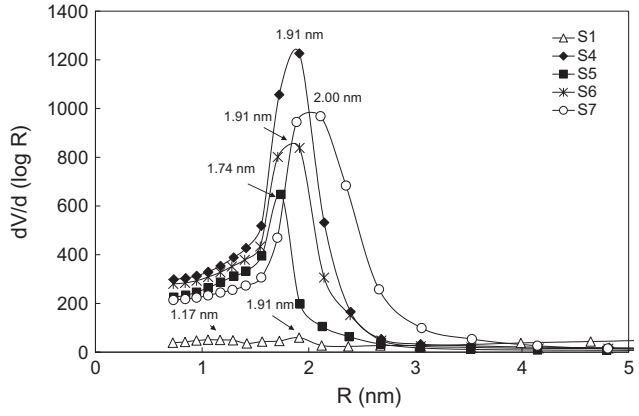

Fig. 5. Pore size distribution of samples synthesized by mixtures of CTAT and Pluronic F127 in alkaline conditions. The molar composition of gels is tabulated in Table 1.

the binding between the polymer and silicate anions is stronger than the counterion-mediated charge coupling between the cationic surfactant and silicate [35]. It may be concluded that this effect combined with the low affinity between Pluronic F127 and CTAT, and the high α values, causes that the addition of the silica precursor probably promotes a demixing of micelles, giving a low-curvature structure similar to that produced, as an example, by CTAB in alkaline conditions [24] and therefore small mesopores. The strong difference between the microscopic structure of sample S7 and samples S4–S6 arises from the differences between the surfactants responsible of the structure (CTAT and Pluronic F127). Pluronic F127 micelles (probably including some CTAT molecules) are thus the main responsible of the small mesopores, which is supported by the existence of the same pores in sample S7.

On the other hand, it is also known that the size of mesopores is strongly dependent on the temperature of the Pluronic-TEOS mixture before (called synthesis temperature) and during (called aging temperature) hydrothermal treatment [36]. According to the work of Zhao et al. [9], higher temperatures result in larger pore sizes and thinner silica walls. In agreement with Zhao and co-workers, Ballem et al. [37] reported an increase in pore size (from 3.8 to 4.1 nm) and a decrease in wall thickness (from 10.7 to 8.5 nm) in SBA-16 silicas by increasing the synthesis temperature from 1 to 40 °C. The authors attributed it to the temperature-dependent hydrophilicity of the PEO block of the copolymer. Resulting PEO moieties are expected to interact more strongly with the silica species and thus be more closely associated with the inorganic wall than the more hydrophobic PPO block. However, at higher temperatures, the PEO blocks become more hydrophobic due to the dehydration of its chains, resulting in increased hydrophobic domain volumes (or in decreased hydrophilic corona volumes), smaller lengths of PEO segments associated with the silica wall, and increased pore sizes [9,37,38]. The temperature of synthesis used in this work was room temperature (25 ± 2 °C).

3.4. Acidic synthesis of silica materials using CTAT–Pluronic F127 system as template

Fig. 8 shows the pore size distribution of samples synthesized by mixtures of CTAT and Pluronic F127 in acidic conditions. The inclusion of the triblock copolymer leads to smaller pores having a narrower distribution in comparison with the pure CTAT system, which is attributed to the presence of free Pluronic F127 micelles in the system, although the effect of synthesis temperature (temperature of mixtures before hydrothermal treatment) should not be discarded. Table 1 and SM Table S3 show the main data obtained from nitrogen adsorption–desorption isotherms, and SEM and TEM, respectively. All nitrogen sorption isotherms (data not shown) were type IV with the hysteresis loop H2, similar to that of sample S3 (Fig. 4d).

Fig. 9 shows the electron micrographs of samples synthesized by mixtures of CTAT and Pluronic F127 in acidic conditions. On the one hand, the macroscopic structure is monolithic, and the microscopic one varies from spheres in samples S3 and S8, to finely granular in samples S9 and S10 as shown in Fig. 9a and b, respectively. On the other hand, all samples having the triblock copolymer show small nearly round pores, as shown in the TEM micrograph (Fig. 9c).

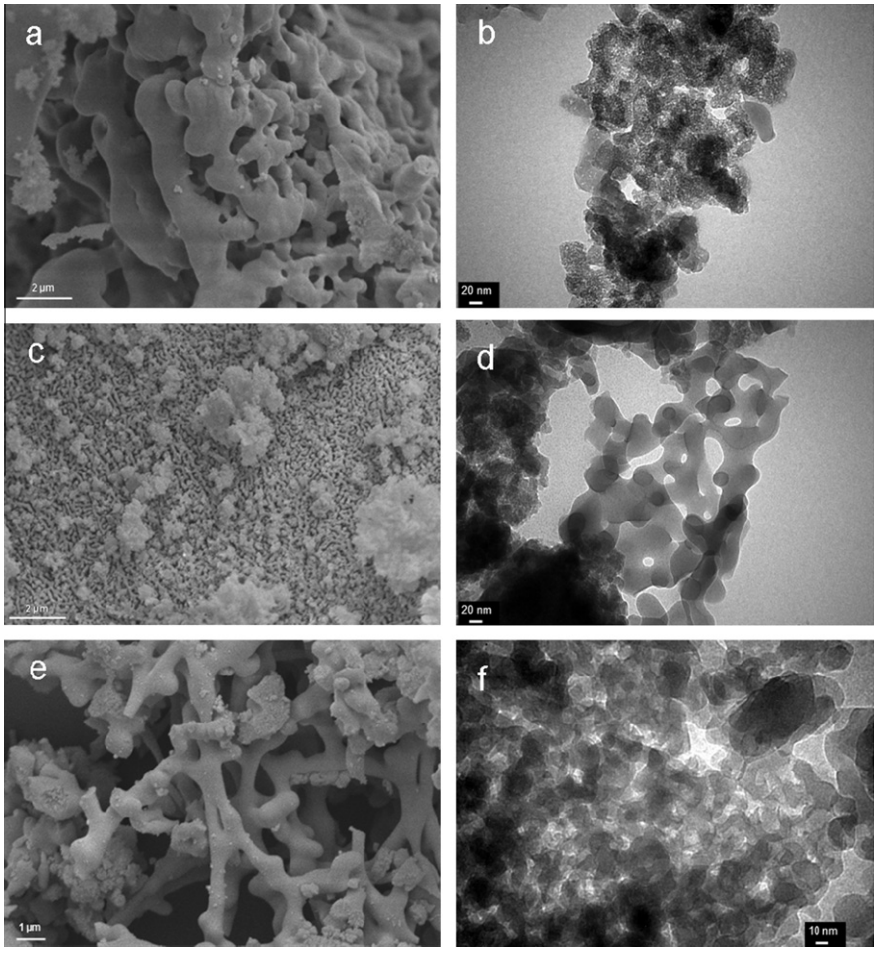

Fig. 6. SEM (20,000×, left side) and TEM (200,000×, right side) micrographs of: (a, b) S5, (c, d) S6, and (e, f) S7.

All samples are monolithic, and the microscopic structure of the sample having higher proportion of CTAT is globular as in the pure CTAT system. However, increasing the Pluronic F127 content, the spheres disappear and the structure becomes finely granular in both S9 and S10 samples. This suggests that in sample S8, the release of the cationic surfactant from mixed aggregates is high enough to produce the same microscopic structure as in pure CTAT system, but this is not the case in sample S9. Changes in morphology on the silica materials by varying the ionic surfactant/triblock copolymer molar ratio can also be observed by analyzing data reported by Poyraz et al. [39], who studied the synthesis of mesoporous silicas by using mixed CTAB–Pluronic P85 surfactants as templates. In fact, the authors reported that at high CTAB/Pluronic P85 M ratio, the excess CTA^+ ions go to the air–water interface to produce mesostructured silica films as well as using pure CTAB, which supports the results obtained in this work. On the other hand, nearly round pores observed in all samples having the triblock copolymer can be interpreted, as in the alkaline samples, as created by Pluronic F127 micelles or Pluronic–CTAT complexes.

3.5. Alkaline synthesis of silica materials using CTAT–Pluronic F68 system as template

SM Fig. S1 shows the pore size distribution of samples synthesized by mixtures of CTAT and Pluronic F68 in alkaline conditions. As well as in CTAT–Pluronic F127, the inclusion of Pluronic F68 in the system produces a change from the bimodal pore size distribution of the mesoporous silica to a broad monomodal distribution of mesopores. Table 1 and SM Table S4 show the main data obtained from nitrogen sorption isotherms, and SEM and TEM, respectively.

The nitrogen sorption isotherm on S11 and S14 (data not shown) are type IV similar to that of sample S1. The hysteresis loop is type H3, typical of plate-like particles giving rise to slit-shaped mesopores [22]. However, samples S12 and S13 show type IV isotherms similar to that of Fig. 7a but with a more pronounced step at $P/P_0 = 0.28$ (S12) and $P/P_0 = 0.33$ (S13). This is interpreted as a stepwise multilayer adsorption on a uniform non-porous surface. The step-height represents the monolayer capacity for each adsorbed layer [22]. Similar isotherms were found in some MCM-41 materials [23]. Then, the monolayer capacity of systems synthesized with CTAT–Pluronic F68 is higher than that in the systems CTAT–Pluronic F127.

Electron micrographs, shown in Fig. 10, reveal that all the samples having Pluronic F68 are formed by spheres, which in turn are formed by agglomerations of amalgamated porous smaller spheres. Large spheres are isolated in sample S11 and S12 (Fig. 10a and b), but form a monolithic bicontinuous structure in sample S13 and S14. The bicontinuous microstructure of sample S14 is different from that of S13, the former being smoother than the latter (Fig. 10c–e).

Zhao et al. [10] reported the synthesis of a mesoporous silica by using a cubic mesophase of Pluronic F68 in alkaline conditions which gave a material having $A_{BET} = 700\ m^2\ g^{-1}$, $D_{aBJH} = 3.50$ nm, and $V_{BJHdepv} = 0.36\ cm^3\ g^{-1}$ and whose microscopic structure was formed by ropelike aggregates. Our material has lower surface area and pore volume, but higher pore size (see Table 1), and maintains

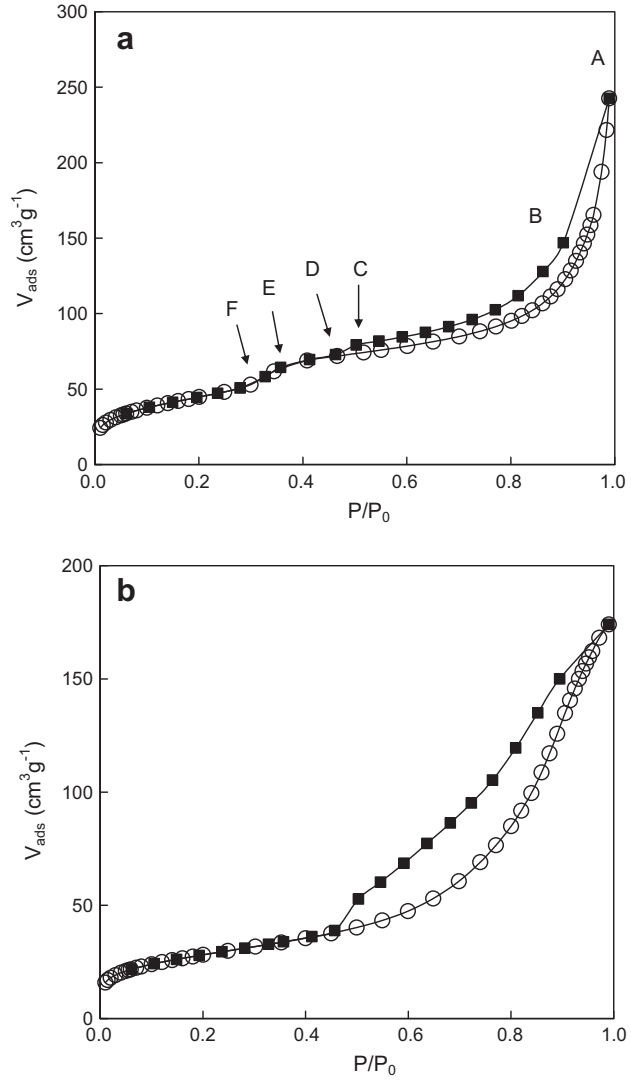

Fig. 7. Nitrogen sorption isotherms on (a) S6 and (b) S7. Open circles, adsorption; and solid squares, desorption.

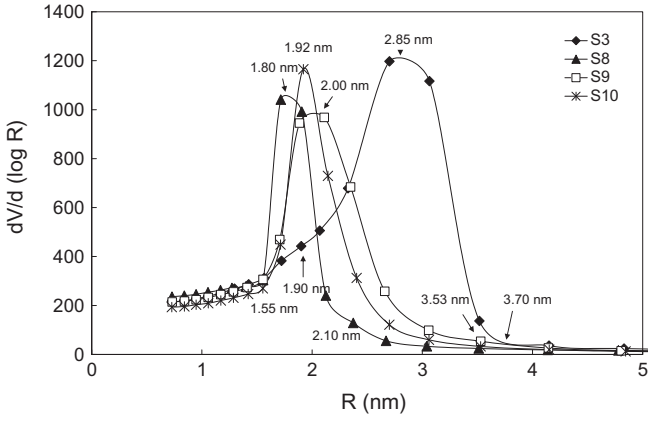

Fig. 8. Pore size distribution of samples synthesized by mixtures of CTAT and Pluronic F127 in acidic conditions. The molar composition of gels is tabulated in Table 1.

the microscopic structure (see Fig. 10e). The differences may be caused, as well as in the CTAT–Pluronic F127 system, by the dissimilar concentration of the template and the unlike gelation conditions. TEM micrographs of all samples having F68 show small platelets with slit pores, similar to that of sample S1 (Fig. 2c).In a previous work [17], we found that the interaction between CTAT and Pluronic F68 is different from that between CTAT and Pluronic F127. The structure of Pluronic F68 micelles is only slightly modified with respect to that existing in pure state, while the neighbors of CTAT micelles in the mixed aggregates are very different from those in pure cationic surfactant micelles. In the CTAT–Pluronic F68 system, there is repulsion below $\alpha_{CTAT} \approx 0.25$, while an attractive interaction occurs at higher CTAT contents. At $\alpha_{CTAT} \approx 0.85$, there is a minimum, indicating that the maximum attraction between components occurs. When $X^m_{CTAT} > 0.75$ (X^m_{CTAT} being the mole fraction of CTAT in the mixed micelles without considering the solvent), a structural transformation of aggregates occurs, which differs strongly from both pure CTAT and pure Pluronic F68 micelles. Pluronic F68 molecules are saturated with $n_{CTAT} \approx 7.5$. As in CTAT–Pluronic F127 systems, the ionization degree of micelles is high, but lower than in the later system. Moreover, in the cyclic voltammetry study measurements [34], there is an increase in the hydrodynamic radius of CTAT–F68 aggregates by increasing the CTAT content, except for $\alpha_{CTAT} = 0.85$ ($X_{CTAT} = 0.82$), in which there is a reduction of R_h from about 10 nm to about 1 nm. For sample S11, $\alpha_{CTAT} = 0.90$ and $\alpha = 0.43$, for S12, $\alpha_{CTAT} = 0.85$ and $\alpha = 0.39$, and for S13, $\alpha_{CTAT} = 0.50$ and $\alpha = 0.54$. This indicates that the polar head groups of cetyltrimethylammonium ions are closer in CTAT–Pluronic F68 micelles than in CTAT–Pluronic F127 ones.

The divergences between the silica materials obtained using CTAT–Pluronic F127 and CTAT–Pluronic F68 systems as templates may be explained from the differences in the properties of the respective mixed aggregates: while in CTAT–Pluronic F127 systems, there is a repulsive interaction between the components, thus facilitating de-mixing by the interaction between micelles of the template and silica precursors, the interaction is attractive in the system CTAT–Pluronic F68, and then, it is probable that the mixture acts as a unique complex. CTAT may interact with the block copolymer molecules through hydrogen bonding and strong van der Waals forces between the oxyethylene group of Pluronic F68 and the head group of CTA^+ ions. Similar interactions were reported by Liu et al. [40] in the system CTAB–Pluronic P123. Again, the alkaline medium is the mainly factor that promotes a low-curvature structure in some of the systems (S1, S13 and S14). The effect was also observed in systems with non-ionic surfactants as template, such as Triton X-100 [31].

3.6. Acidic synthesis of silica materials using CTAT–Pluronic F68 system as template

SM Fig. S2 shows the pore size distribution of samples synthesized by mixtures of CTAT and Pluronic F68 in acidic conditions. As well as in the CTAT–Pluronic F127 system, the inclusion of Pluronic F68 leads to smaller pores having a narrower distribution than in the pure CTAT system, which are probably formed by copolymer or copolymer–CTAT mixed micelles at room temperature. Moreover, Bahadur et al. [41] found that F68 micelles are less compact and more solvated than those formed by the more hydrophobic members of the Pluronics family. Thus, in this case, it is possible that the PEO chains be more or less fully extended into solution enabling silica penetration deep into the micelle corona prior to the heating step, to result in such small pores. The nitrogen sorption isotherms of all samples (data not shown) are similar to that of sample S3 (Fig. 4d); i.e., they are type IV with a H2 hysteresis loop which corresponds to a non-defined distribution of pore sizes and shapes, as discussed above [22]. Table 1 and SM Table S5 show the main data obtained from nitrogen adsorption isotherms, and SEM and TEM, respectively.

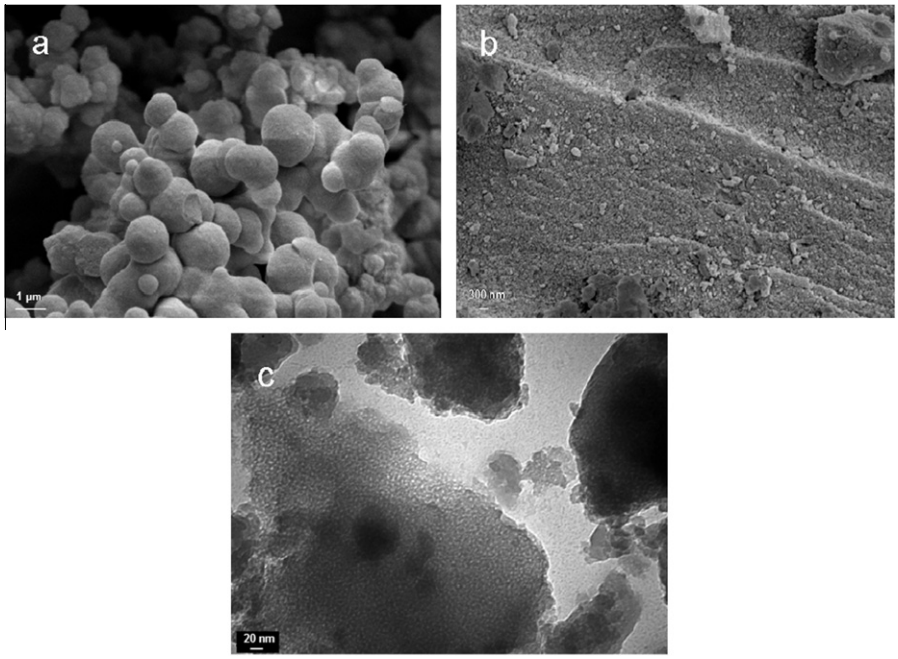

Fig. 9. Electron micrographs of materials synthesized by mixtures of CTAT and Pluronic F127 in acidic conditions: (a, b) SEM micrographs of samples S8 and S9, respectively (magnitude = 20,000×); and (c) TEM micrograph of sample S8 (magnitude = 200,000×).

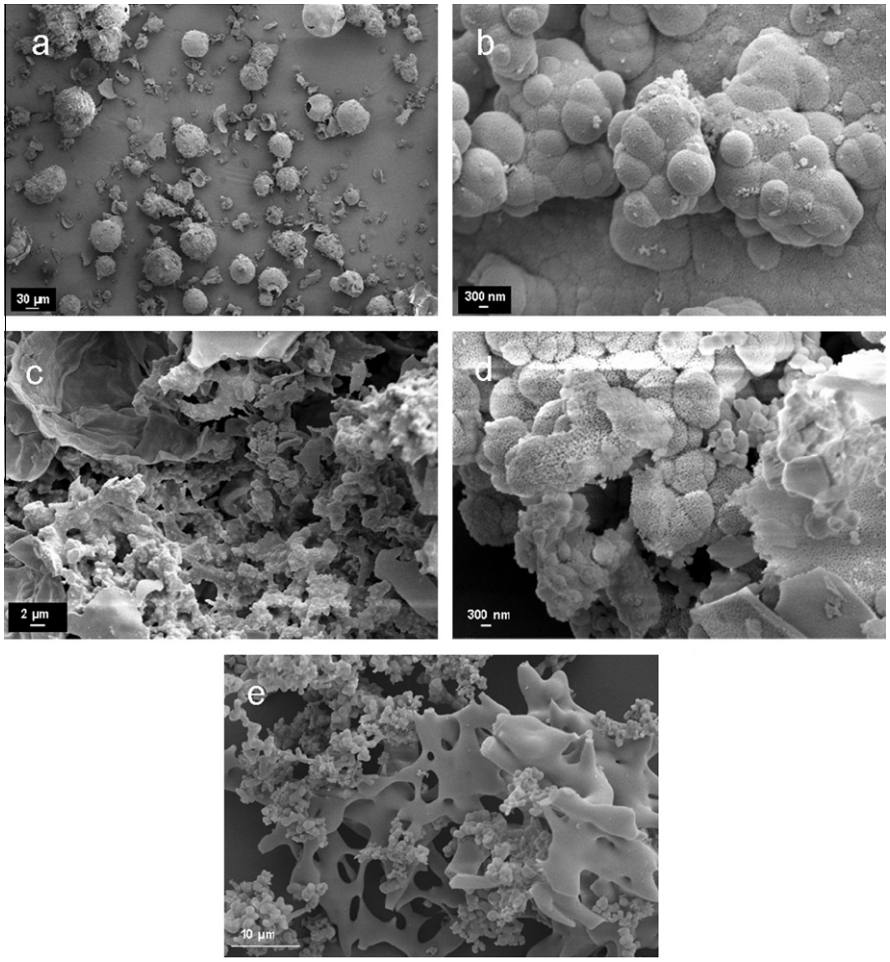

Fig. 10. SEM micrographs of materials synthesized by mixtures of CTAT and Pluronic F68 in alkaline conditions: (a) S11 (300×), (b) S12 (20,000×), (c) S13 (5000×), (d) S13 (19,000×), and (e) S14 (5000×).

Please cite this article in press as: M. Brigante, P.C. Schulz, J. Colloid Interface Sci. (2011), doi:10.1016/j.jcis.2011.11.056

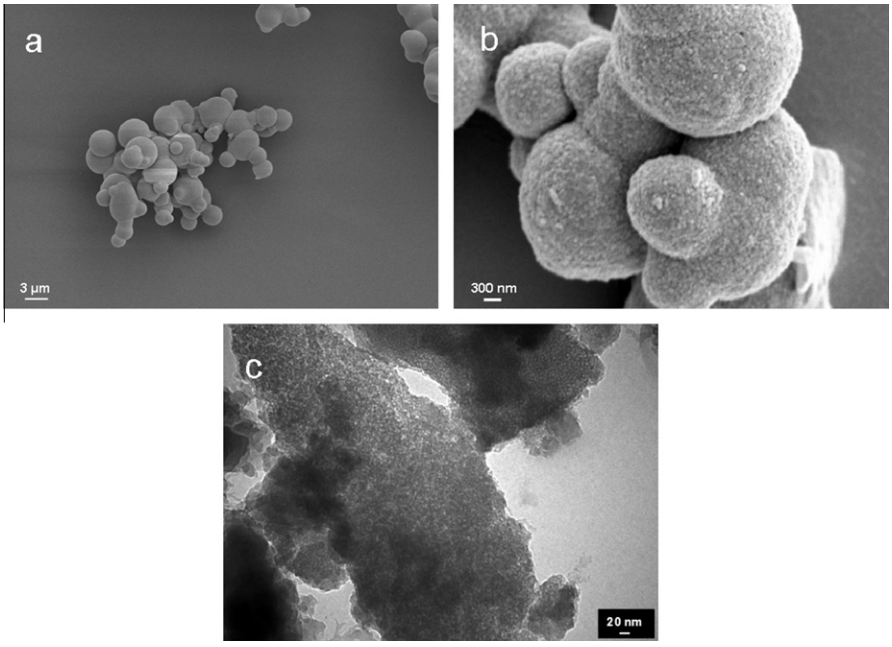

Fig. 11. Electron micrographs of materials synthesized by mixtures of CTAT and Pluronic F68 in acidic conditions: (a, b) SEM micrographs of samples S15 (5000×) and S17 (40,000×), respectively, and (c) TEM micrograph of sample S17 (200,000×).

Fig. 11 shows the microscopic aspect of samples S15–S17. These materials consist of agglomerates of polydisperse spheres (Fig. 11a). At higher magnifications (Fig. 11b), they show a sandy granular aspect. At very high magnification (Fig. 11c), the sandy texture shows irregular mesopores, having a pore diameter $D_{pore} \approx 3.80$ nm.

The obtained results indicate that the microscopic texture of these samples is only governed by the synthesis pH, independently on the surfactant composition, i.e., samples S3 and S15–S17 have spheroidal shape. The mesoporous structure seems to indicate that, as mentioned above, the CTAT–Pluronic F68 mixed micelles act as stable entities to template the silica. As determined in a previous work [17], their mixed micelles do not differ significantly from Pluronic F68 pure micelles, as it is reflected in the almost invariant mesopore size in samples S15–S17.

4. Conclusions

Our results reveal that the structure of the silica materials was affected by the acidity or alkalinity of the synthesis gel, but also by the characteristics of the interaction between the surfactants in the template. Using pure CTAT, microscopic bicontinuous materials are obtained in alkaline synthesis, which are composed by nanoscopic plate-like particles having slit-shaped pores. Strong electrostatic interactions between silanolate groups and cationic surfactant ions seem to be the main factor that controls the synthesis mechanism. In acidic synthesis, on the contrary, monolithic silicas are obtained. These materials are also composed by nanoscopic plate-like particles having slit-shaped pores, although in some cases, the microscopic structures are formed by fused spherical particles. The synthesis mechanism is attributed to a weaker electrostatic interaction throughout a bridge counterion at the interface between the surfactant and the cationic silica precursor.

The inclusion of Pluronic triblock copolymers to the CTAT–TEOS system produces materials with small and nearly round pores. Besides, there are changes in morphology and texture of the materials, which are attributed not only to the synthesis pH and temperature but also to the interaction between CTAT and Pluronic F127 (mainly repulsive) and between CTAT and Pluronic F68 (mainly attractive). On the one hand, bicontinuous platelets having slit-shaped mesoporous are obtained in alkaline synthesis by using CTAT–Pluronic F127 as template; while all materials showed monolithic (spheres or granular) structure in acidic media. On the other hand, bicontinuous polydisperse spheres having plate-like slit pores are formed by using CTAT–Pluronic F68 as template, independently on the synthesis pH conditions.

The obtained results have a significant importance in several processes, where the control of the pH, surfactant concentration, and ionic surfactant/triblock copolymer molar ratio (within others) in the production of synthetic materials can play a key role. Taking into account this concept, one can design a convenient and economic path for getting the mesoporous products to match the desired applications. Based on our results, silica materials synthesized at acidic pH and at high CTAT/Pluronic F127 M ratio (or at low CTAT/Pluronic F68 M ratio) have higher surface area and pore volume than at alkaline pH, which would be desirable in some adsorption and catalysis applications. On the contrary, silica materials synthesized at alkaline pH have higher D_{aBJH} values (see Table 1), which would be desirable in, for example, biomolecular encapsulation and controlled drug release. Big pore sizes could also be obtained at temperature of synthesis higher than 25 °C, in agreement with several works reported in literature [9,37,38]. On the other hand, the results can be helpful to continue future investigations about understanding copolymer–(ionic or non-ionic) surfactant interactions, because it is not only an academic interest, but it is also important (such as shown in this work) from the application point of view. In fact, there is desirable to explore these interactions by using other compounds of the Pluronic family to correlate these with the resulting mesoporous materials properties.

Acknowledgment

This work was supported by a grant of the Universidad Nacional del Sur and other by the Agencia Nacional de Promoción Científica y Técnica de la República Argentina (ANPCyT). M. Brigante thanks CONICET for the postdoctoral fellowship.

Appendix A. Supplementary material

Supplementary data associated with this article can be found, in the online version, at doi:10.1016/j.jcis.2011.11.056.

References

[1] M. Mesa, L. Sierra, J. Patarin, J.L. Guth, Solid State Sci. 8 (2005) 990.
[2] J.Y. Ying, C.P. Mehnert, M.S. Wong, Angew. Chem. Int. Ed. 38 (1999) 56.
[3] C.T. Kresge, M.E. Leonowicz, W.J. Roth, J.C. Vartuli, J.S. Beck, Nature 359 (1992) 710.
[4] H.P. Lin, C.Y. Mou, Acc. Chem. Res. 35 (2002) 927.
[5] J. Wang, C.K. Tsung, R.C. Hayward, Y. Wu, G.D. Stucky, Angew. Chem. Int. Ed. 44 (2005) 332.
[6] K. Flodström, H. Wennerström, C.V. Teixeira, H. Amenitsch, M. Linden, V. Alfredsson, Langmuir 20 (2004) 10311.
[7] H. Chen, J. He, Chem. Commun. (2008) 4422.
[8] L. Sierra, S. Valange, J.L. Guth, Micropor. Mesopor. Mater. 124 (2009) 100.
[9] D. Zhao, J. Feng, Q. Huo, N. Melosh, G.H. Fredrickson, B.F. Chmelka, G.D. Stucky, Science 279 (1998) 548.
[10] D. Zhao, Q. Huo, J. Feng, B.F. Chmelka, G.D. Stucky, J. Am. Chem. Soc. 120 (1998) 6024.
[11] Y. Sakamoto, I. Díaz, O. Terasaki, D. Zhao, J. Pérez-Pariente, J.M. Kim, G.D. Stucky, J. Phys. Chem. B 106 (2002) 3118.
[12] Z. Jin, X. Wang, X. Cui, Micropor. Mesopor. Mater. 108 (2008) 183.
[13] Y.K. Hwang, K. Rangu Patil, S.H. Jhung, J.S. Chang, Y.J. Ko, S.E. Park, Micropor. Mesopor. Mater. 78 (2005) 245.
[14] J. Li, Q. Hu, H. Tian, C. Ma, L. Li, J. Cheng, Z. Hao, S. Qiao, J. Colloid Interface Sci. 339 (2009) 160.
[15] C.J. Brinker, G.W. Scherer, Sol–Gel Science, Academic Press, San Diego, 1990.
[16] L. Qi, J. Ma, H. Cheng, Z. Zhao, Chem. Mater. 10 (1998) 1623.
[17] M. Brigante, P.C. Schulz, J. Surf. Deterg. 14 (2011) 439.
[18] M.T. Truong, L.M. Walker, Langmuir 16 (2000) 7991.
[19] J. Mata, D. Varade, P. Bahadur, Thermochim. Acta 428 (2005) 147.
[20] P.V. Messina, M.A. Morini, M.B. Sierra, P.C. Schulz, J. Colloid Interface Sci. 300 (2006) 270.
[21] J.F.A. Soltero, J.E. Puig, O. Manero, P.C. Schulz, Langmuir 11 (1995) 3337.
[22] K.S.W. Sing, D.H. Everett, R.A.W. Haul, L. Moscou, R.A. Pierotti, J. Rouquérol, T. Siemieniewska, Pure Appl. Chem. 57 (1985) 603.
[23] G. Lelong, S. Bhattacharyya, S. Kline, T. Cacciaguerra, M.A. Gonzalez, M.L. Saboungi, J. Phys. Chem. C 112 (2008) 10674.
[24] Y. Liu, A. Karkamkar, T.J. Pinnavaia, Chem. Commun. (2001) 1822.
[25] K.W. Gallis, C.C. Landry, Chem. Mater. 9 (1997) 2035.
[26] A.J. Müller, M.F. Torres, A.E. Sáez, Langmuir 20 (2004) 3838.
[27] B.A. Schubert, E.W. Kaler, N.J. Wagner, Langmuir 19 (2003) 4079.
[28] M.R. Rojas, A.J. Müller, A.E. Sáez, J. Colloid Interface Sci. 326 (2008) 221.
[29] L.D. Mendoza, M. Rabelero, J.I. Escalante, E.R. Macías, A. González-Álvarez, F. Bautista, J.F.A. Soltero, J.E. Puig, J. Colloid Interface Sci. 320 (2008) 290.
[30] M.A. Morini, R.M. Minardi, P.C. Schulz, J.E. Puig, M.E. Hernandez-Vargas, Colloids Surf. A 103 (1995) 37.
[31] L. Sierra, B. López, J.L. Guth, Micropor. Mesopor. Mater. 39 (2000) 519.
[32] H. Huo, D.I. Margolese, U. Ciesia, P. Feng, T.E. Gier, P. Sieger, R. Leon, P.M. Petroff, F. Schüth, G.D. Stucky, Nature 368 (1994) 317.
[33] H.P. Lin, S.T. Wong, C.Y. Mou, C.Y. Tang, J. Phys. Chem. B 104 (2000) 8967.
[34] E.N. Schulz, R. Ambruzzi, S.G. García, M. Brigante, J. Colloid Interface Sci., submitted for publication.
[35] M.G. Song, J.Y. Kim, S.H. Cho, J.D. Kim, Langmuir 18 (2002) 6110.
[36] T. Klimova, A. Esquivel, J. Reyes, M. Rubio, X. Bokhimi, J. Aracil, Micropor. Mesopo. Mater. 93 (2006) 331.
[37] M.A. Ballem, J.M. Córdoba, M. Odén, Micropor. Mesopor. Mater. 129 (2010) 106.
[38] C.F. Cheng, Y.C. Lin, H.H. Cheng, Y.C. Chen, Chem. Phys. Lett. 382 (2003) 496.
[39] A.S. Poyraz, C. Albayrak, Ö. Dag, Micropor. Mesopor. Mater. 115 (2008) 548.
[40] C. Liu, S. Wang, Z. Rong, X. Wang, G. Gu, W. Sun, J. Non-Cryst. Solids 356 (2010) 1246.
[41] P. Bahadur, P. Li, M. Almgren, W. Brown, Langmuir 8 (1992) 1903.